Vegetation on mesic loamy and sandy soils along a 1700-km maritime Eurasia arctic transect

Walker, Donald A ; Epstein, Howard E ; Šibík, Jozef ; Bhatt, Uma ; Romanovsky, Vladimir E ; Breen, Amy L ; Chasnikova, Silvia ; Daanen, Ronald ; Druckenmiller, Lisa A ; Ermokhina, Ksenia ; Forbes, Bruce C ; Frost, Gerald V ; Geml, Jozsef ; Kaärlejarvi, Elina ; Khitun, Olga ; Khomutov, Artem ; Kumpula, Timo ; Kuss, Patrick ; Matyshak, Georgy ; Moskalenko, Natalya ; Orekhov, Pavel ; Peirce, Jana ; Raynolds, Martha K ; Timling, Ina

Abstract: Questions How do plant communities on zonal loamy vs. sandy soils vary across the full maritime Arctic bioclimate gradient? How are plant communities of these areas related to existing vegetation units of the European Vegetation Classification? What are the main environmental factors controlling the transitions of vegetation along the bioclimate gradient? Location 1700-km Eurasia Arctic Transect (EAT), Yamal Peninsula and Franz Josef Land (FJL), Russia. Methods The Braun-Blanquet approach was used to sample mesic loamy and sandy plots at 14 total study sites at six locations, one in each of the five Arctic bioclimate subzones and the forest-tundra transition. Trends in soil factors, cover of plant growth forms (PGFs), and species diversity were examined along the summer-warmth-index (SWI) gradient and on loamy and sandy soils. Classification and ordination were used to group the plots and to test relationships between vegetation and environmental factors. Results Clear, mostly nonlinear, trends occurred for soil factors, vegetation-structure, and species diversity along the climate gradient. Cluster analysis revealed seven groups with clear relationships to subzone and soil texture. Clusters at the ends of the bioclimate gradient (forest-tundra and polar desert) had many highly diagnostic taxa, whereas clusters from the Yamal Peninsula had only a few. Axis 1 of a Detrended Correspondence Analysis was strongly correlated with latitude and summer warmth; Axis 2 was strongly correlated with soil moisture, percentage sand, and landscape age. Conclusions Summer temperature and soil texture have clear effects on tundra canopy structure and species composition, with consequences to ecosystem properties. Each layer of the plant canopy has a distinct region of peak abundance along the bioclimate gradient. The major vegetation types are weakly aligned with described classes of the European Vegetation Checklist indicating a continuous floristic gradient rather than distinct subzone regions. The study provides ground-based vegetation data for satellite-based interpretations of the western maritime Eurasian Arctic, and the first vegetation data from Hayes Island, Franz Josef Land, which is strongly separated geographically and floristically from the rest of the gradient and most susceptible to ongoing climate change.

DOI: https://doi.org/10.1111/avsc.12401

Originally published at:
Walker, Donald A; Epstein, Howard E; Šibík, Jozef; Bhatt, Uma; Romanovsky, Vladimir E; Breen, Amy L; Chasnikova, Silvia; Daanen, Ronald; Druckenmiller, Lisa A; Ermokhina, Ksenia; Forbes, Bruce C; Frost, Gerald V; Geml, Jozsef; Kaärlejarvi, Elina; Khitun, Olga; Khomutov, Artem; Kumpula, Timo; Kuss, Patrick; Matyshak, Georgy; Moskalenko, Natalya; Orekhov, Pavel; Peirce, Jana; Raynolds, Martha K; Timling, Ina (2019). Vegetation on mesic loamy and sandy soils along a 1700-km maritime Eurasia arctic transect. Applied Vegetation Science, 22(1):150-167.
DOI: https://doi.org/10.1111/avsc.12401

PROF. DONALD A. WALKER (Orcid ID : 0000-0001-9581-7811)

Article type : Synthesis

Coordinating Editor: Dr. Borja Jiménez-Alfaro

Vegetation on mesic loamy and sandy soils along a 1700-km maritime Eurasia Arctic Transect

Donald A. Walker, Howard E. Epstein, Jozef Šibík, Uma Bhatt, Vladimir E. Romanovsky, Amy L. Breen, Silvia Chasnikova, Ronald Daanen, Lisa A. Druckenmiller, Ksenia Ermokhina, Bruce C. Forbes, Gerald V. Frost, Jozsef Geml, Elina Kaärlejarvi, Olga Khitun, Artem Khomutov, Timo Kumpula, Patrick Kuss, Georgy Matyshak, Natalya Moskalenko, Pavel Orekhov, Jana Peirce, Martha K. Raynolds, & Ina Timling

Walker, D.A. (Corresponding author, dawalker@alaska.edu)[1]

Epstein, H.E. (hee2b@virginia.edu)[2]
Šibík, J. (jozef.sibik@savba.sk)[3]
Bhatt, U.S. (usbhatt@alaska.edu)[4]
Romanovsky, V.E. (veromanovsky@alaska.edu)[4]
Breen, A.L. (albreen@alaska.edu)[5]
Chasníková, S. (chasnikova.silvia@gmail.com)[3]
Daanen, R. (ronald.daanen@alaska.gov)[6]
Druckenmiller, L.A. (ladruckenmiller@alaska.edu)[1]
Ermokhina, K. (diankina@gmail.com)[7]
Forbes, B.C. (bruce.forbes@ulapland.fi)[8]
Frost, G.V. (jfrost@abrinc.com)[9]
Geml, J. (jozsef.geml@naturalis)[10]
Kaärlejarvi, E. (elina.kaarlejarvi@emg.umu.se)[11]
Khitun, O. (khitun-olga@yandex.ru)[12]
Khomutov, A. (akhomutov@gmail.com)[7, 13]
Kumpula, T. (timo.kumpula@uef.fi)[14]
Kuss, P. (patrick.kuss@systbot.uzh.ch)[15]
Matyshak, G. (matyshak@gmail.com)[16]
Moskalenko, N. (nat-moskalenko@mail.ru)[7]
Orekhov, P. (orekhov.eci@gmail.com)[7]
Peirce, J. (jlpeirce@alaska.edu)[1]

This article has been accepted for publication and undergone full peer review but has not been through the copyediting, typesetting, pagination and proofreading process, which may lead to differences between this version and the Version of Record. Please cite this article as doi: 10.1111/avsc.12401

Raynolds, M.K. (mkraynolds@alaska.edu)[1]
Timling, I. (itimling@alaska.edu)[1]

[1]Alaska Geobotany Center, Institute of Arctic Biology & Department of Biology and Wildlife, University of Alaska, Fairbanks, AK, United States, 99709
[2]Department of Environmental Sciences, University of Virginia, Charlottesville, Virginia, 22904, United States
[3]Plant Science and Biodiversity Center, Slovak Academy of Sciences, Institute of Botany, Dúbravská cesta 9, 845 23, Bratislava, Slovak Republic
[4]Geophysical Institute & Department of Atmospheric Science, University of Alaska, Fairbanks, Alaska, United States, 99709
[5]International Arctic Research Center, University of Alaska, Fairbanks, Alaska, United States, 99709
[6]Division of Geological & Geophysical Surveys, 3354 College Road, Fairbanks, Alaska, United States, 99709
[7]Earth Cryosphere Institute, Tyumen Scientific Center, Russian Academy of Sciences, Siberian Branch, 86 Malygin street, Tyumen, 625026, Russia
[8]Arctic Center, University of Lapland, PL 122, 96191, Rovaniemi, Finland
[9]Alaska Biological Research, Inc., P.O. Box 80410, Fairbanks, Alaska, Fairbanks, AK, United States, 99708
[10]Naturalis Biodiversity Center, Darwinweg 2, 2333 CR Leiden, The Netherlands
[11]Department of Ecology and Environmental Sciences, Umeå University, 901 87, Umeå, Sweden
[12]Komarov Botanical Institute, Russian Academy of Sciences, Professor Popova Street, 2, St. Petersburg, 197376, Russia
[13]University of Tyumen, 6 Volodarsky St., Tyumen, 625003, Russia
[14]University of Eastern Finland, Yliopisokatu 2, FI-80100, Joensuu, Finland
[15]Institute of Systematic and Evolutionary Botany, University of Zürich Zollikerstrasse 107 8008, Zürich, Switzerland
[16]Department of Soil Science, Lomonosov Moscow State University, Leninskie Gory, 119992 Moscow, Russia

Abstract

Questions: How do plant communities on zonal loamy vs. sandy soils vary across the full maritime Arctic bioclimate gradient? How are plant communities of these areas related to existing vegetation units of the European Vegetation Classification? What are the main environmental factors controlling the transitions of vegetation along the bioclimate gradient?

Location: 1700-km Eurasia Arctic Transect (EAT), Yamal Peninsula and Franz Josef Land (FJL), Russia.

Methods: The Braun-Blanquet approach was used to sample mesic loamy and sandy plots at 14 total study sites at six locations, one in each of the five Arctic bioclimate subzones and the forest-tundra transition. Trends in soil factors, cover of plant growth forms (PGFs), and species diversity were examined along the summer-warmth-index (SWI) gradient and on loamy and sandy soils. Classification and ordination were used to group the plots and to test relationships between vegetation and environmental factors.

Results: Clear, mostly nonlinear, trends occurred for soil factors, vegetation-structure, and species diversity along the climate gradient. Cluster analysis revealed seven groups with clear relationships to subzone and soil texture. Clusters at the ends of the bioclimate gradient (forest-tundra and polar desert) had many highly diagnostic taxa, whereas clusters from the Yamal Peninsula had only a few. Axis 1 of a Detrended Correspondence Analysis was strongly correlated with latitude and summer warmth; Axis 2 was strongly correlated with soil moisture, percentage sand, and landscape age.

Conclusions: Summer temperature and soil texture have clear effects on tundra canopy structure and species composition, with consequences to ecosystem properties. Each layer of the plant canopy has a distinct region of peak abundance along the bioclimate gradient. The

major vegetation types are weakly aligned with described classes of the European Vegetation Checklist indicating a continuous floristic gradient rather than distinct subzone regions. The study provides ground-based vegetation data for satellite-based interpretations of the western maritime Eurasian Arctic, and the first vegetation data from Hayes Island, Franz Josef Land, which is strongly separated geographically and floristically from the rest of the gradient and most susceptible to ongoing climate change.

Keywords

Arctic; Bioclimate subzones; Braun-Blanquet classification; aboveground biomass, DCA ordination; Nomalized Difference Vegetation Index (NDVI), plant growth forms, remote sensing; soil texture; summer warmth index; tundra biome

Nomenclature

Pan-Arctic Species List (PASL) (Raynolds et al., 2013), which is a circumpolar compendium of accepted names for vascular plants (Elven, Murray, Razzhivin, & Yurtsev, 2011), mosses (Belland, 2012), liverworts (Konstantinova & Bakalin, 2009), and lichens (Kristinsson, 2010).

Abbreviations:

CAVM, Circumpolar Arctic Vegetation Map; DCA, Detrended Correspondence Analysis; EAT, Eurasia Arctic Transect; EVC, European Vegetation Classification; LAI, leaf-area index; NDVI, Normalized Difference Vegetation Index; PGF, plant growth form; SWI_a, Summer Warmth Index of the atmosphere at 2-m; SWI_g, Summer Warmth Index at the ground surface.

Introduction

Arctic tundra ecosystems occur in a broad circumpolar belt that extends from areas north of 80 ˚N to forest-tundra areas south of 60 ˚N, with mean July temperatures that vary from near 0 ˚C to over 12 ˚C. Several conceptual approaches have been used to subdivide the vegetation along the broad bioclimate gradients of Eurasia (Alexandrova, 1980; Chernov & Matveyeva, 1997; Yurtsev, 1994a), North America (Bliss, 1997; Daniëls, Bültmann, Lünterbusch, & Wilhelm, 2000; Edlund, 1990; Polunin, 1951), and the circumpolar Arctic (Elvebakk, Elven, & Razzhivin, 1999; Tuhkanen, 1984; D. A. Walker et al., 2005; Yurtsev, 1994b). Only a few studies, however, have attempted to examine continuous vegetation transitions of zonal plant communities along transects that traverse the full Arctic bioclimate gradient because of the rather daunting logistics involved. Examples exist for the Taymyr Peninsula, Russia (Matveyeva, 1998), the North America Arctic Transect (NAAT) (D. A. Walker, Kuss, et al., 2011b), and the 1999 Canada transect for the Circumpolar Arctic Vegetation Map (Gonzalez, Gould, & Raynolds, 2000). Arctic alpine vegetation gradients have been described along elevation gradients in the mountains of southwestern Greenland (Sieg, Drees, & Daniëls, 2006).

Here we describe the vegetation along the 1700-km Eurasia Arctic Transect (EAT) that includes the Yamal Peninsula and Franz Josef Land (Fig. 1). The aim is to characterize vegetation on zonal loamy and sandy soils along the complete maritime Arctic climate gradient in western arctic Russia to aid in remote-sensing interpretations of land-cover and land-use change (D. A. Walker, Epstein, et al., 2012a). The zonal patterns, geological conditions, permafrost, and summer-thaw depth (active layer) conditions are generally well described along the length of the peninsula. We analyze the variations in plant growth forms and species richness in each layer of the plant canopy with respect to summer temperature and soil texture, present a preliminary numerical classification, and use indirect ordination methods to analyze the relationship of the plots and species to a suite of measured environmental factors.

Methods

Site selection and sampling

We established the EAT during four expeditions in the summers of 2007–2010 (Fig. 1). The transect extends from the Krenkel Hydro-meteorological Station on Hayes Island (80˚ 37’ N, 58˚ 03’ E) in the maritime polar desert of Franz Josef Land, to Nadym (65˚ 19’ N, 72˚ 53’ E) in the forest-tundra transition of West Siberia. Mean July temperatures range from 1 ˚C at the northern end of the transect to 15.8˚C at the southern end. Six study locations were selected along the EAT to represent zonal (Razzhivin, 1999; Walter, 1954; 1973) vegetation conditions in each of the five Arctic bioclimate subzones and the forest-tundra transition, as mapped on the Circumpolar Arctic Vegetation Map (D. A. Walker et al., 2005; Yurtsev, 1994b) (Table 1). At each location we chose at least two study sites — one on mesic loamy soils and one on mesic sandy soils (See Supplementary Information, Appendix S1 for geological setting in relationship to soils).

We used the Braun-Blanquet approach (Westhoff & Van der Maarel, 1978) to sample mesic loamy and sandy sites at each location. At most study sites there was adequate space for a large relatively homogeneous 50 m x 50 m sample site that corresponded approximately to the 30-m to 70-m pixel size of the Landsat satellite sensors. Sample plots and transects were arranged in the pattern shown in Supplementary Information, Appendix S2. Here we describe the data mainly from 5 m x 5 m (25 m^2) plots, except at the Nadym forest site, where 10 m x 10 m (100 m^2) plots were used, and the Nadym tundra site, where 1 m x 1 m (1 m^2) plots were used to sample homogeneous areas of vegetation on patterned-ground features (earth hummocks). We sampled 79 plots, but eliminated three Nadym wetland plots, resulting in a final dataset of 76 plots, distributed among the six EAT locations: Krenkel (KR, 10 plots), Ostrov Belyy (BO, 20 plots), Laborovaya (LA, 10 plots), Kharasavey (KH, 10 plots), Vaskiny Dachi (VD, 15 plots), and Nadym (ND, 11 plots) (see Supplemental Information, Appendix S3 for descriptions and photographs of the study sites.)

Each vascular plant, bryophyte and lichen species occurring within a plot was recorded and a sample taken as a voucher. Unknown species were sent to the Komarov Botanical Institute (KBI) for final identification. The cover-abundance of each species was recorded using Braun-Blanquet categories (r = single occurrence; + = several occurrences but < 1 % cover; 1 = 1–5 %

cover; 2 = 6–25 %; 3 = 26–50 %; 4 = 51–75 %; 5 = 76–100 %) (Braun-Blanquet, 1928). For calculating the mean cover, the cover-abundance scores were transformed to a mean percentage score corresponding to the midpoint of each cover-abundance category: r = 0.05; + = 0.5; 1 = 2.5; 2 = 15; 3 = 37.5; 4 = 62.5; 5 = 87.5. Plant species were also assigned to plant-growth-form (PGF) categories (Supplemental Information, Appendix S4).

The environmental data from each plot include 107 variables, including site, soil, biomass, spectral data, NDVI, and canopy structure variables. (see details in Supplemental Information, Appendices S5.1 and S5.2, and the project data reports (D. A. Walker, Carlson, et al., 2011a; D. A. Walker et al., 2008a; D. A. Walker, Epstein, et al., 2009a; D. A. Walker, Orekhov, et al., 2009b).

Soils samples were collected from the uppermost mineral-soil horizons at a point just outside the southwest corner of each vegetation plot. Larger soil pits were dug just outside the southwest corner of the 50 x 50-m grid to fully describe vertical and horizontal variation in the soil profiles. The pits were described by Dr. Georgy Matyshak according the Russian approach and translated into descriptions corresponding to the US Soil Taxonomy approach (Soil Survey Staff, 1999) and are included with photographs in the data reports cited above.

Climate

The Arctic bioclimate zonation patterns portrayed on the Circumpolar Arctic Vegetation Map (CAVM Team, 2003) are based primarily on summer temperature regimes and structure of the vegetation (Yurtsev, 1978, 1994a). We use the summer warmth index (SWI), which is the sum of monthly mean temperatures above 0 ˚C, measured in ˚C mo "thawing-degree months". The SWI is calculated from monthly mean temperature data and is very strongly correlated with thawing--degree days, which require daily mean temperature to calculate. SWI is equivalent to the warmth index, *a*, used by Steve Young for the vascular-plant flora of St. Lawrence Island, Alaska (Young, 1971). Four of the six EAT locations have long-term climate-station data; for these locations, we calculated the SWI for air temperatures (SWI_a) at the standard 2-m height of weather-station observations. To obtain consistent summer temperature data for all study locations over the same length of record, we used data from the thermal infrared channels of satellite-based Advanced Very High Resolution Radiometers (AVHRR, 1982-2003) (Comiso, 2003; 2006) to calculate SWI_g, the ground-surface summer warmth index (SWI_g) within 12.5-km pixels containing the study locations (Bhatt et al., 2010). Consistent data for other climate factors, such as precipitation and wind, were not available across all study locations.

Vegetation analysis

Cluster analysis

We used a hierarchical dendrogram approach, available in PC-ORD to group the plots into clusters based on the similarity of their species compositions (McCune, Grace, & Urban, 2002) via the JUICE 7.0 software (Tichý, 2002). The most meaningful separation of the 76 plots was achieved with the flexible-beta group linkage method (β = -0.25) with the Sørensen distance measure and square root data transformation. We included species-level taxonomic

determinations in the analyses, and we excluded taxa that were identified only to the genus level. To determine the optimal number of clusters providing the highest 'separation power' for the dataset, we used the Crispness of Classification approach (Z. Botta-Dukát, Chytrý, & Hájková, 2005) available through the Optimclass function in JUICE (Tichý, 2002). A synoptic table was prepared using the combined synoptic table function in JUICE. Taxa with high fidelity (modified phi coefficients ≥ 0.5) were interpreted as diagnostic for the group; taxa with modified phi coefficients ≥ 0.8 were interpreted as highly diagnostic.

Analysis of vegetation and environmental variables

We compared the trends of plant-growth-form (PGF) cover along the bioclimate gradient (SWI_g) for each layer of the plant canopy (tree and shrub layer, herb layer, and cryptogam layer); and the species richness within groups of dominant PGFs (deciduous shrubs, evergreen shrubs, graminoids, forbs, mosses, lichens). We also examined trends of soil properties along the bioclimate gradient.

Ordination

We explored several ordination methods available in the R program (R Development Core Team, 2013) through the JUICE vegetation analysis package (Tichý, 2002). Detrended Correspondence Analysis (DCA) (Hill & Gauch, 1980) provided the clearest, most easily interpreted separation of plots along complex environmental gradients. Plot and species similarities were calculated using the Sørenson similarity index. Rare species were downweighted and the axes scaled according to the program defaults. The four main DCA axes 1, 2, 3, and 4 were correlated with continuous and ordinal environmental variables in each plot using species-environment correlations in the program CONOCO via JUICE. Only variables with $p \leq 0.002$ determined by global permutation test with forward selection (number of permutations: 499) are shown in the biplot diagrams.

Results

Descriptions of the EAT locations and study sites

An overview of the study-sites (Table 1) includes the study locations, coordinates, bioclimate subzones, study-site numbers, geological setting, parent material, field plot numbers, and dominant vegetation. Descriptions and photos of the environment and vegetation of each study location and study site are in Supplemental information, Appendix S3. The species and environmental data from the 79 sample plots are in Appendices S4 and S5.

Mean July temperatures range from 1 ˚C at Krenkel to 15.8 ˚C at Nadym. Mean annual precipitation ranges from 258 mm at Ostrov Belyy to 479 mm at Nadym (Table 2). The SWI_g values at the EAT study locations are generally within one standard deviation of the circumpolar SWI_g means of bioclimate subzones B to E (Table 2, columns 6 and 7), which indicates that these locations are representative of the mean zonal summer temperature conditions. The exception is Krenkel (SWI_g = 2 ˚C mo), which is much colder than the mean SWI_g for subzone A (8.2 ± 3.4 ˚C mo). The 12.5-km pixels of the satellite-derived SWI_g are subject to subpixel effects arising from the contrasting temperature regimes of different

surfaces, especially near glaciers and coastlines (Smith, Reynolds, Peterson, & Lawrimore, 2008); however, the satellite-derived SWI_g values are within 1 ˚C mo of the station SWI_a values at all EAT study locations where station data are available, including the three coastal locations, (Table 2, columns 5 and 3).

Clay, silt, and sand percentages for loamy and sandy sites are shown using the US Department of Agriculture soil texture triangle (Fig. 2a). Loamy sites had 19–61 % sand and 31–62 % silt. Sandy sites generally had >80 % sand, and <20 % silt. Clay percentages were low (<25 %) at all sites. On the loamy sites, silt and clay percentage were somewhat higher in the central part of the summer-temperature gradient. Sand percentages were higher at both ends of the gradient (Fig. 2b).

Classification and syntaxonomical interpretation

The cluster analysis dendrogram shows the progressive linkage of plots according to their floristic similarity (Fig. 3). Clusters with higher levels of similarity are toward the left side of the diagram. Crispness of Classification identified two clusters with the highest level of separability (dissimilarity). One cluster contained all of the Yamal plots (subzones B, C, D, & E) and the other contained all the plots of FJL (subzone A) and Nadym (FT transition). The next highest level of dissimilarity was achieved with six clusters, separated at the level of the red dashed line in Figure 3. At this level, clusters 5 and 6 in Figure 3 were joined, forming one large cluster containing most of the plots on the Yamal Peninsula, including the subzone D loamy plots, all subzone C plots, and the subzone B loamy plots. Based on our knowledge of the rather unique floristic character of the loamy subzone B site, which has characteristics similar to the moist nonacidic tundra described from North America, Greenland and Russia, we shifted the breakpoint for cluster definition slightly to the left so that the subzone B loamy plots were recognized as a separate cluster, resulting in a final grouping with seven clusters.

A synoptic table (Table 3) shows the frequency of species with very high fidelity (modified phi ≥ 0.8) and high fidelity (0.8 > modified phi ≥ 0.5). The full synoptic table, including diagnostic and non-diagnostic taxa, is in Supplementary Information, Appendix S6. Lists of the diagnostic, frequent, and dominant taxa in each cluster are in Supplementary Information, Appendix S7. A summary of the contents of the clusters and their alignment with described Br.-Bl. syntaxa (mostly classes) are as follows:

Cluster 1 contains the five forest plots at Nadym with five highly diagnostic taxa (phi ≥ 0.8; *Pinus sylvestris, Betula pubescens, Larix sibirica, Vaccinium myrtillus, Juniperus communis*) and six other diagnostic taxa (phi ≥ 0.5). This cluster aligns with Cl. *Vaccinio–Piceetea* and All. *Vaccinio uliginosi–Pinion sylvestris* Br.-Bl. in Br.-Bl. et al. 1939, which contains Holarctic coniferous and boreo-subarctic birch forests on oligotrophic and leached soils in the boreal zone (Mucina et al., 2016).

Cluster 2 contains the six tundra plots in the forest-tundra transition at Nadym with three highly diagnostic taxa (*Carex globularis, Andromeda, polifolia, Rubus chamaemorus*) and one other diagnostic taxon (*Rhododendron tomentosum*) This cluster aligns with Cl. *Oxycocco–Sphagnetea* Br.-Bl. et Tx. ex Westhoff et al. 1946, which contains dwarf-shrub, sedge and peat-moss vegetation of the Holarctic ombrotrophic bogs and wet heath on extremely acidic soils.

Cluster 3 contains all 10 plots in subzone A at Krenkel. This is the most distinctive cluster with 13 highly diagnostic taxa (*Stellaria edwardsii, Papaver dahlianum, Phippsia algida, Cochlearia groenlandica, Lecidea ramulosa, Orthothecium chryseum, Cladonia pocillum, Cetraria delisei*) and 18 other diagnostic taxa. Many of these are diagnostic for the recently described "polar desert" Br.-Bl. class *Drabo corymbosae–Papaveretea dahlilani* (Daniëls, Elvebakk, Matveyeva, & Mucina, 2016), which contains cushion forb, lichen, moss tundra occurring in polar deserts of the Arctic zone of the Arctic Ocean archipelagos (Mucina et al., 2016).

Clusters 4, 5, 6, and 7 form a broad group of plots across the central part of the Yamal Peninsula with a general trend from relatively warm sites in cluster 4 (subzones E and D) to relatively cold sites in clusters 6 and 7 (subzone B). Although all four clusters have several diagnostic taxa (phi>0.5), there are only three highly diagnostic taxa (phi≥0.8) in the group. **Cluster 4** contains the ten subzone E plots at Laborovaya and the five sandy plots in subzone D at Vaskiny Dachi. It has one highly diagnostic taxon (*Flavocetraria nivalis*) and eight other diagnostic taxa. This cluster aligns weakly with Cl. *Oxycocco–Sphagnetea* Br.-Bl. et Tx. ex Westhoff et al. 1946, which contains dwarf-shrub, sedge and peat-moss vegetation of the Holarctic ombrotrophic bogs and wet heath on extremely acidic soils (Mucina et al., 2016). **Cluster 5** contains the 10 subzone D loamy plots and 10 subzone C plots. It has eight diagnostic taxa (*Lophozia ventricosa, Alopecurus borealis, Salix reptans, Eriophorum angustifolium*, *Tephroseris atropurpurea, Peltigera canina, P. aphthosa, Lichenomphalia hudsoniana*), and no highly diagnostic taxa. This cluster weakly aligns with Cl. *Scheuchzerio palustris–Caricetea fuscae* Tx. 1937, which contains sedge-moss vegetation of fens, transitional mires, and bog hollows in the temperate, boreal and Arctic zones (Mucina et al., 2016). **Cluster 6** contains the five loamy plots at Ostrov Belyy, each of which has two micro-habitat subplots corresponding to nonsorted circles and inter-circle areas. It has one highly diagnostic taxon (*Blepharostoma trichophyllum*) and eight other diagnostic taxa (*Salix polaris, Tomentypnum nitens, Dryas octopetala, Poa arctica, Juncus biglumis Bryum cyclophyllum, Stellaria longipes, Sphenolobus minutus*). This cluster weakly aligns with Cl. *Carici rupestris-Kobresietea bellardii* Ohba 1974, which contains, circum-Arctic fellfield and dwarf-shrub graminoid tundra on base-rich substrates (Mucina et al., 2016). It has characteristics of plant communities occurring on moist nonacidic soils in Alaska [Ass. Dryado integrifoliae–Caricetum bigelowii (M. D. Walker, Walker, & Auerbach, 1994)], Greenland [*Eriophorum angustifolium–Rhododendron lapponicum* comm. (Lünterbusch & Danie ls, 2004)], and the Taimyr Peninsula, Russia [Carici arctisibiricae–Hylocomietum alaskana (Matveyeva, 1994)]. **Cluster 7** contains the 10 subzone B sandy plots at Belyy Ostrov. It has one highly diagnostic taxon (*Pogonatum dentatum*) and 12 other diagnostic taxa (*Oxyria digyna, Gymnomitrion corallioides, Luzula confusa, Salix nummularia, Lloydia serotina, Solorina crocea, Polytrichum piliferum, Pohlia crudoides, Gowardia nigricans*). This cluster very weakly aligns

with Cl. *Saxifrago cernuae–Cochlearietea groenlandicae* Mucina et Daniëls 2016, which contains vegetation of open graminoid tundra disturbed by cryoturbation (Mucina et al., 2016).

Soils, vegetation structure, and species richness

Trends of key soil and key vegetation-canopy factors (canopy layer height, litter, standing dead, LAI, NDVI, total phytomass) vs. SWI_g are in Supplemental Information, Appendix S8.

Soil properties that increase with higher SWI_g include percentage of sand (on sandy sites), thickness of organic horizons, percentage soil carbon (on loamy sites), and active layer thickness (Supplemental Information, Table S8-1). Soil properties that tend to decrease with SWI_g include soil pH, soil moisture, and sodium concentration. Loamy sites have generally higher volumetric soil moisture, pH, cation exchange capacity (CEC), sodium, volumetric soil moisture, thicker organic soil horizons, more soil carbon and nitrogen, and shallower thaw depth.

The height of the plant canopy, number of canopy layers, LAI, NDVI, and total phytomass all generally increase with summer warmth (Supplemental Information, Table S8.2, and Fig. 4). The only site with trees is the Nadym forest site (ND1), which has mean total tree cover of 26% (Fig. 4a, left, brown portion of stacked bars), split between evergreen-needleleaf trees (*Pinus sylvestris* and *P. sibirica*), deciduous broadleaf trees (*Betula pubescens*), and deciduous needleleaf trees (*Larix sibirica*). (See Supplemental Information, Appendix S4 for the raw species cover estimates.) Low shrubs (40–200 cm tall) occur in subzones D and E and the forest-tundra (VD1, VD2, LA1, LA2, ND1, and ND2) and are most abundant on loamy soils (Fig. 4a, left). Dwarf shrubs (<40 cm tall) occur in all subzones except subzone A, where woody plants are absent. Deciduous-shrub cover (Fig. 4a, center) varies nearly linearly with SWI_g on loamy soils ($R^2 = 0.91$) and has a weak polynomial trend ($R^2 = 0.38$) on sandy soils. Evergreen-shrub cover has an exponential trend on loamy soils ($R^2 = 0.89$) and sandy soils ($R^2 = 0.61$) (Fig. 4a, right). Deciduous- and evergreen-shrub height and LAI increase exponentially with SWI_g (Supplemental Information, Figure S8-2).

Graminoids are dominant in the herbaceous layer in all subzones except subzone A, where forbs are most abundant (Fig. 4b, left). Graminoid cover peaks at 40% in subzone D on loamy soils (Fig. 4b center). On sandy soils, graminoid cover peaks at approximately 20% in subzones C and E. Sedges dominate the graminoid cover in all subzones except subzone A, where sedges are absent. Sedges have generally higher cover on loamy sites compared to sandy sites. Grass cover is highest (exceeding 14%) on loamy soils in subzones C and D. Forbs occur with low cover in all subzones except subzone A, where they are the dominant component of the vascular-plant cover (Fig. 4b, right).

Lichens peak at both ends of the gradient on both loamy and sandy sites (Fig. 4c, left and right). Fruticose lichens have highest cover in subzone E and the forest-tundra transition, exceeding 60% cover on loamy and sandy sites in the forest-tundra transition (ND1 & ND2); whereas, crustose lichens (including biological crusts) have highest cover in subzone A, exceeding 80% cover on loamy and sandy sites (KR1 & KR2). Pleurocarpous mosses (those with branching growth forms, often forming carpets) are more abundant on loamy soils; whereas acrocarpous mosses (unbranched, often smaller mosses) are more abundant on acidic soils. Bryophyte cover peaked in the central part of the SWI_g gradient.

The range in total species richness at seven of the twelve sites was 39–46 species per plot, with extremes of 19.8 species per plot at the FT-forest loamy site and 56 species per plot at the subzone B loamy site (Supplemental Information, Appendix S10 and Fig. 4d, left). The low species richness at the FT-forest site (ND-1) is explained by the low diversity of cryptogams (6.2 lichen species and 3 bryophyte species), despite the very high cover of fruticose reindeer lichens. The high species richness at the subzone B loamy site (BO-1) is partly due to the presence of patterned-ground and two distinct microhabitats (nonsorted-circle centers and inter-circle areas) within the 5 x 5-m plots.

The mean species richness is high in the cryptogam layer (lichens plus bryophytes, gray and brown lines in Fig. 4d, center and right), ranging between 25–47 species per plot at all sites except for ND-1, which has 9.2 species per plot. The average total species richness ranges much more narrowly between 7.8 and 13.8 in the herb and shrub layers (Fig. 4d). The various PGFs reach their peak mean richness at different points along the bioclimate and texture gradients: Lichens, 26.8 species/plot (subzone E, sandy); bryophytes, 23.6 species/plot (subzone B, loamy); forbs, 8.2 species/plot (subzone A, loamy); graminoids, 7.4 species/plot (subzone D, loamy); deciduous shrubs, 4.4 species/plot (subzone E, sandy); evergreen shrubs, 4 species/plot (forest-tundra transition, sandy); and trees, 3.4 species/plot (forest-tundra transition, loamy).

Ordination

The DCA plot ordination (Fig. 5a) displays the 76 plots according to their respective bioclimate subzone, texture class, and cluster. Axis 1 has a high positive linear correlation with latitude (0.96) and a high negative correlation with SWI_g (-0.77). Plots in Subzone A (cluster 3) are geographically and floristically widely separated from plots in the rest of the clusters, which form a large megacluster toward the left side of the ordination. Within the megacluster, there is generally a clear separation of plots in each of the statistical cluster, with transition from the relatively warm FT sites (clusters 1 and 2) on the left side of the megacluster to the subzone B (clusters 6 and 7) on the right side. There is relatively high floristic similarity among most of the plots in this megacluster, particularly among clusters 4, 5, and 6, indicating a continuous floristic gradient along the main Yamal Peninsula, rather than distinct vegetation units in each bioclimate subzone. Axis 2 has a strong positive correlation with sand percentage (0.64) and a strong negative correlation with soil moisture and terrace age (-0.75 and 0.51 respectively). All sandy sites (colored squares) are in the upper part the ordination, and loamy sites (colored circles) are in the lower part.

The species ordination (Fig. 5b) displays the centroids of distribution of five taxa with the highest fidelity to each of the seven clusters (35 total taxa). As expected, the centers of distributions for the diagnostic taxa generally align with the areas of the clusters for which they are diagnostic.

Discussion and conclusions

Mesic vegetation transitions along the EAT summer temperature gradient

A primary motivation for this study was to develop a baseline of ground-based vegetation information along the complete Arctic summer-temperature gradient in the maritime Arctic portion of western Russia to support remote-sensing interpretations. We sampled and analyzed plant communities on homogeneous mesic sites with loamy and sandy soils along the summer-temperature gradient of the EAT. Satellite-derived summer land-surface temperatures (Comiso, 2006; Raynolds, Comiso, Walker, & Verbyla, 2008) provided a consistent spatial record of mean summer ground-surface temperatures (SWI_g) across the full length of the EAT, including locations where station data were unavailable.

The EAT analysis focused on mesic tundra areas where climate is the primary factor controlling the character of the vegetation. Although we initially considered these mesic sites to be zonal habitats, it soon became clear that the tundra over nearly the entire Yamal Peninsula is strongly influenced by a long history of reindeer grazing. The only locations that were free of recent reindeer foraging were Nadym and Krenkel. Both these sites had high cover of lichens, indicating that reindeer at the other sites have greatly reduced the lichen cover. Reindeer herds graze heavily on lichens particularly during the snow-covered months of winter and spring. The results of our study and others (Pajunen, 2009; Pajunen, Virtanen, & Roininen, 2008; Vowles, Lovehav, Molau, & Björk, 2017; Yu, Epstein, Walker, Frost, & Forbes, 2011) and comparison with results from a similar transect in North America where there are relatively low *Rangifer* densities (D. A. Walker, Epstein, et al., 2012a) indicate that the reindeer have had a long-term major impact to the shrub, graminoid and moss layers on the Yamal (Forbes et al., 2009). Quantifying this effect is difficult because of lack of reindeer exclusion areas.

Vegetation units described here for the middle portion of the EAT bioclimate gradient display gradual floristic transitions between bioclimate subzones and are only weakly aligned with previously described Br.-Bl. classes. A formal association-level classification for the Yamal region should await a broader analysis that includes new data collected within the past few years. Data from both the EAT and NAAT transects and additional data from zonal sites elsewhere in the Arctic should be used to develop a unified Braun-Blanquet classification for zonal vegetation across the full Arctic bioclimate gradient using the habitat-based approach of Mucina et al. (2016) (Walker et al., 2018). There is especially a need for new Br.-Bl. class corresponding to zonal acidic tundra in the middle part of Arctic bioclimate gradient. Additional studies are needed to develop clear Br.-Bl. syntaxa to characterize the variation along other important habitats and environmental gradients across the Arctic, including representative toposequences, riparian chronosequences, snowbed gradients, and major disturbance gradients.

The analyses of trends PGF cover and richness within canopy layers vs. mean SWI_g provided quantitative data across the bioclimate gradient that support the observations of other investigators including: (1) the occurrence of progressively more and taller layers in the plant canopy with warmer temperatures (Elmendorf et al., 2012; Matveyeva, 1998), (2) increases in vascular-plant cover and diversity along the summer temperature gradient (Daniëls et al., 2013; Rannie, 1986; Young, 1971), and (3) exclusion of woody plants, sedges, and *Sphagnum* peat from the northernmost subzone A (Yurtsev, 1994b). While cover and species richness of evergreen- and deciduous-shrubs generally increased with higher SWI_g, cover of lichens, and forbs declined. Graminoid cover and species richness of lichens and bryophyte species richness showed parabolic trends with maximum values in the central part of the temperature gradient.

Much recent research regarding productivity patterns in the Arctic has focused on the increased abundance of shrubs associated with warming temperatures, which are thought to be a primary cause of the recent increases in NDVI observed in satellite data (Myers-Smith et al., 2011). Our study documented strong, mostly positive exponential trends with SWI_g for deciduous-and evergreen-shrub cover, shrub-layer height, herb-layer height, litter cover, LAI, NDVI, and aboveground phytomass. The study also documented the dominance of shrubs in the Low Arctic (subzones E and D), dwarf shrubs, graminoids, and bryophytes in the Middle Arctic (subzones C and B), and forbs and crustose lichens in the extreme High Arctic.

The role of soil texture

The floristic contrast between the loamy and sandy sites varies considerably between locations across the EAT, a result of much great site-factor heterogeneity of the sandy sites. The Nadym and Ostrov Belyy locations illustrate rather extreme contrasts in ecosystem structure that can occur on loamy vs. sandy soils. At Nadym, the site on the sandy relatively young surface at ND-1 is relatively well drained, has no permafrost, and is forested; whereas the ND-2 site on older more-fine grained soils is ice-rich, relatively poorly drained, and covered with hummocky tundra vegetation (Supplemental Information, Appendix S3, Fig. S3-6). A host of site factors interact to affect the vegetation structure and composition at this site, including much thicker soil organic layers, thin active layers, relatively cold soils, and very low CECs on the older loamy soils. A similar contrast occurred at Ostrov Belly (Appendix S3, Fig. S3-2) and it is illustrated in the numerical classification and DCA ordination, where the sandy and loamy plots are placed in separate clusters (6 and 7) (Fig. 3) and are widely separated along Axis 2 of the ordination (Fig. 5). (Figs. 3 and 5). The sandy sites at Ostrov Belyy are much drier than the loamy sites at this location and have many other site-factor differences that separate them.

The opposite situation occurs at Krenkel (subzone A, Appendix S3, Fig. S3-2), where both study sites have similar site factors with high floristic similarity and are placed in a single tight cluster in the ordination (cluster 3, Figs. 3 and 5). Loamy and sandy sites at Laborovaya (subzone E, Appendix S3, Fig. S3-5) also have high floristic similarity, but in this case, there is also relatively high similarity with the sandy sites at Vaskiny Dachi (Fig. S3-4), so all three sites (LA-1, LA-2, VD-2,) are placed in a single numerical cluster (cluster 4, Figs, 3 and 5), with several acidophilic, oligotrophic, hypoarctic diagnostic species.

Part of the explanation for much larger variation in the sandy sites, is that during site selection, it was relatively easy to find large sites to sample vegetation on mesic silt loam to sandy loam soils, whereas the availability of mesic very sandy sites was more limited. The relatively young sandy sites are also more susceptible to disturbance by reindeer and strong winds, whereas the older loamy sites have tended to stabilize toward the regional zonal conditions.

Special importance of subzone A

A major accomplishment of this study was the first detailed vegetation description from exceptionally cold, wet, and windy Hayes Island. Our results documented the high floristic dissimilarity of Hayes Island to the rest of the EAT (Fig. 5), the dominance of biological soil crusts in the cryptogam layer, and the dominance of forbs among the vascular plants (Fig. 4b). It revealed a vegetation composed mainly of biological soil crusts, where even the vascular plants in the herb layer have cryptogam-like cushion and mat growth forms, unlike any other site along the EAT. Sites not exposed to excessive wind erosion had unexpectedly high hand-held NDVI (0.44–0.48) most likely caused by the high cover of wet biological soil crusts, which covered 50–85% of the soil surface and composed 33–86% of the total biomass (D. A. Walker, Frost, et al., 2012b). Rich fruticose-lichen communities occurred on the most favorable zonal sites on Hayes Island, a result of the absence of reindeer (Supplemental Information, Appendix S12).

Numerous other studies have also noted the unique vegetation in subzone A (Chernov & Matveyeva 1997; Daniëls, et al. 2016) and its extreme susceptibility to climate change (Walker, et al., 2008). It is interesting that the total species richness of coldest, most northern location (Krenkel, 37 species) of the warmest most southern location (Nadym, 20 species) (Supplemental Information, Appendix S12). The relatively high species richness at Krenkel is due to the large number of cryptogam species (24–27.8 species). Other arctic researchers have also noted high plot-scale cryptogam species richness at cold temperatures (Matveyeva1998; Lünterbusch & Daniëls 2004; Bültmann 2005; Timling et al. 2012). In studies of Arctic lichen floras from subzone E to subzone A, the number of vascular-plant species declines by approximately 95 percent, whereas the number of lichen species declines by only approximately 15 percent (Dahlberg & Bültmann 2013). The same authors note that the relatively small decline in lichen species at higher latitudes is due mainly to reductions in the numbers of lichens that normally grow on woody plants, which are greatly reduced toward the north. Increased availability of light due to reduced competition from herbs and shrubs is a major cause of high moss and lichen richness at the more northern sites (Marshall & Baltzer, 2015; M. D. Walker et al., 2006). Further competition for light occurs within very dense cryptogam layers in the southern locations, where a few reindeer lichen species with erect fruticose-lichen growth forms (e.g. *Cladonia stellaris*, *C. stygia, C. rangiferina*, *C. arbuscula*, and *C. mitis*) densely cover the ground of lichen woodlands and outcompete other species.

Implications for Arctic climate change and ecosystem studies

Ground-based documentation of existing patterns of vegetation is a critical element of space-based monitoring of changes to terrestrial ecosystems during a time of rapid climate and land-use change in the Arctic (Stow et al., 2004). The patterns of vegetation greenness (NDVI) change

have not been spatially nor temporally consistent across the Arctic, due in part to the constantly changing patterns of sea ice in the Arctic basin (Bhatt et al., 2013) and changes in the growing season and productivity patterns ((Park et al., 2016). Although difficult logistics limit the number of sampling locations and the quantity of data that can be collected in the vast landscapes of the Arctic, there were advantages of these constraints during our studies because they facilitated interdisciplinary teamwork at the selected sites, assuring that a largely spatially coherent database of vegetation, soil, permafrost, and remote-sensing information to aid remote-sensing interpretations and vegetation-change modeling along a full maritime Arctic climate gradient. The research sites are permanently marked and provide a baseline against which to measure future vegetation change. The data should prove useful for interpretations of change to a wide variety of ecosystem properties and functions, including shrub growth (Myers-Smith et al., 2011), permafrost regimes (Romanovsky et al., 2017), Arctic tree lines (Harsch, Hulme, McGlone, & Duncan, 2009), snow distribution (Brown et al., 2017), regional hydrology (Prowse et al., 2017), soil-carbon fluxes (Christensen et al., 2017), biodiversity (Meltofte, 2013), and land-use changes (AMAP 2010; Nymand & Fondahl 2014). As sea ice retreats, it will be important to continue monitoring the changes from space, and also to continue obtaining ground-based information to document the consequences to the land surface (Bhatt et al., 2014). This is especially important in subzone A, which should be considered an endangered bioclimate subzone (D. A. Walker, Raynolds, & Gould, 2008b).

Acknowledgments

Funding was mainly from the U.S. National Aeronautics and Space Administration, Land-Cover Land-Use Change Program (NASA LCLUC grants NNG6GE00A, NNX09AK56J, and NNX14AD90G) with additional support from the Russian Academy of Science, the U.S. National Science Foundation Arctic Science Engineering and Education for Sustainability (NSF ArcSEES Award No. 1263854), the Bureau of Ocean Energy Management (BOEM), and the Slovak Academy of Science award VEGA 2/0135/16. We especially thank Marina Leibman, who led the Russian investigations and organized the logistics for the EAT expeditions. She and numerous other members of the Earth Cryosphere Institute made this study possible.

References

Alexandrova, V. D. (1980). The Arctic and Antarctic: Their Division into Geobotanical Areas. Cambridge: Cambridge University Press.

Belland, R. (2012). Arctic moss database. Retrieved May 20, 2016, cited in Raynolds, M. K. et al. (2013) The Pan-Arctic Species List (PASL). *Arctic Vegetation Archive Workshop, Krakow, Poland, 14-16 April 2013, CAFF Proceedings Series Report Nr. 10*, 92–95.

Bhatt, U. S., Walker, D. A., Raynolds, M. K., Bieniek, P. A., Epstein, H. E., Comiso, J. C., et al. (2013). Recent declines in warming and vegetation greening trends over pan-Arctic tundra. *Remote Sensing*, *5*, 4229–4254.

Bhatt, U. S., Walker, D. A., Raynolds, M. K., Comiso, J. C., Epstein, H. E., Jia, G., et al. (2010). Circumpolar Arctic tundra vegetation change is linked to sea ice decline. *Earth Interact.*, *14*, 1–20.

Bhatt, U. S., Walker, D. A., Walsh, J. E., Carmack, E. C., Frey, K. E., Meier, W. N., et al. (2014). Implications of Arctic sea ice decline for the Earth system. *Annual Review of Environment and Resources*, *39*, 57–89.

Bliss, L. C. (1997). Arctic Ecosystems of North America. In F. E. Wielgolaski (Ed.), *Polar and Alpine Tundra* (pp. 551–683). Amsterdam.

Botta-Dukát, Z., Chytrý, M., & Hájková, P. (2005). Vegetation of lowland wet meadows along a climatic contenentality gradient in Central Europe. *Preslia*, *77*, 89–111.

Braun-Blanquet, J. (1928). Pflanzensoziologie. Grundzüge der Vegetationskunde. *Biologische Studienbücher* (7 ed.). Berlin.

Brown, R., Schuler, D. V., Bulygina, O., Derksen, C., Luojus, K., Mudryk, L., et al. (2017). Arctic terrestrial snow cover. In AMAP (Ed.), *Snow, Water, Ice and Permafrost in the Arctic (SWIPA) 2017* (pp. 25–64). Oslo, Norway: Arctic Monitoring and Assessment Programme (AMAP).

Chernov, Y. I., & Matveyeva, N. V. (1997). Arctic Ecosystems in Russia. In F. E. Wielgolaski (Ed.), *Polar and Alpine Tundra* (pp. 361–507).

Christensen, T. R., Rysgaard, S., Bendtsen, J., Else, B., Glud, R. N., van Huissteden, K., et al. (2017). Arctic carbon cycling. In AMAP (Ed.), *Snow, Water, Ice and Permafrost in the Arctic (SWIPA) 2017* (pp. 203–218). Oslo, Norway: Arctic Monitoring and Assessment Programme (AMAP).

Chytrý, M., Tichý, L., Holt, J., & Botta-Dukát, J. (2002). Determination of diagnostic species with statistical fidelity measures. *Journal of Vegetation Science*, *13*, 79–90.

Comiso, J. C. (2003). Warming trends in the Arctic from clear sky satellite observations. *Journal of Climate*, *16*, 3498–3510.

Comiso, J. C. (2006). Arctic warming signals from satellite observations. *Weather*, *61*(3), 70. http://doi.org/10.1256/wea.222.05

Daniëls, F. J. A., Elvebakk, A., Matveyeva, N. V., & Mucina, L. (2016). The Drabo corymbosae-Papaveretea dahliani − a new vegetation class of the High Arctic polar deserts. *Hacquetia*, *15*, 5–13. http://doi.org/10.2307/3236190

Daniëls, F. J. A., Gillespie, L. J., Poulin, M., Afonina, O. M., Alsos, I. G., Aronsson, M., et al. (2013). Plants. In *Arctic Biodiversity Assessment* (pp. 310–345). Akureyri, Iceland: Conservation of Arctic Flora and Fauna.

Daniëls, F. J., Bültmann, H., Lünterbusch, C., & Wilhelm, M. (2000). Vegetation zones and biodiversity of the North-American Arctic. *Berichte Der Reinhold-Tüxen-Gesellschaft*, *12*, 131.

Edlund, S. (1990). Bioclimate zones in the Canadian Archipelago. In *Canada's Missing Dimension: Science and History in the Canadian Arctic Islands* (pp. 421–441). Ottawa.

Elmendorf, S. C., Henry, G. H. R., Hollister, R. D., Björk, R. G., Boulanger-Lapointe, N., Cooper, E. J., et al. (2012). Plot-scale evidence of tundra vegetation change and links to recent summer warming. *Nature Climate Change*, *2*(6), 457. http://doi.org/10.1038/nclimate1465

Elvebakk, A., Elven, R., & Razzhivin, V. Y. (1999). Delimitation, zonal and sectorial subdivision of the Arctic for the Panarctic Flora Project. In *The Species Concept in the High North - A Panarctic Flora Initiative* (pp. 375–386). Oslo: The Norwegian Academy of Science and Letters.

Elven, R., Murray, D. F., Razzhivin, V. Y., & Yurtsev, B. A. (2011). Annotated checklist of the panarctic flora (PAF): vascular plants. *National Centre of Biosystematics, Natural History Museum, University of Oslo*.

Forbes, B. C., Stammler, F., Kumpula, T., Meschtyb, N., Pajunen, A., & Kaarlejärvi, E. (2009). High resilience in the Yamal-Nenets social-ecological system, West Siberian Arctic, Russia. *Proceedings of the National Academy of Sciences*, *106*(52), 22041–22048. http://doi.org/10.1073/pnas.0908286106

Gonzalez, G., Gould, W. A., & Raynolds, M. K. (2000). *1999 Canadian transect for the Circumpolar Arctic Vegetation Map*. *AGC Data Report* (p. 89). Fairbanks, AK: University of Alaska Fairbanks.

Harsch, M. A., Hulme, P. E., McGlone, M. S., & Duncan, R. P. (2009). Are treelines advancing? A global meta-analysis of treeline response to climate warming. *Ecology Letters*, *12*(10), 1040–1049. http://doi.org/10.1111/j.1461-0248.2009.01355.x

Hill, M. O., & Gauch, H. G. (1980). Detrended correspondence analysis, an improved ordination technique. *Vegetatio*, *42*, 47–58.

Konstantinova, N. A., & Bakalin, V. A. (2009). Checklist of liverworts (Marchantiophyta) of Russia. *Arctoa*, *18*, 1–64.

Lünterbusch, C. H., & Danie ls, F. J. A. (2004). Phytosociological aspects of Dryas integrifolia vegetation on moist-wet soil in Northwest Greenland. *Phytocoenologia*, *34*(2), 241–270. http://doi.org/10.1127/0340-269X/2004/0034-0241

Marshall, K. E., & Baltzer, J. L. (2015). Decreased competitive interactions drive a reverse species richness latitudinal gradient in subarctic forests. *Ecology*, *96*(2), 461–470. http://doi.org/10.1890/14-0717.1

Matveyeva, N. V. (1994). Floristic classification and ecology of tundra vegetation of the Taymyr Peninsula, northern Siberia. *Journal of Vegetation Science*, *5*, 813–828.

Matveyeva, N. V. (1998). Zonation of plant cover in the arctic (Vol. 21). St. Petersburg: Russian Academy of Science.

McCune, B., Grace, J. B., & Urban, D. L. (2002). Analysis of Ecological Communities. Gleneden Beach, OR: MJM Software Design.

Meltofte, H. (Ed.). (2013). Arctic Biodiversity Assessment: Status and trends in Arctic biodiversity. Akureyri: Conservation of Arctic Flora and Fauna.

Mucina, L., Bültmann, H., Dierßen, K., Theurillat, J.-P., Raus, T., Čarni, A., et al. (2016). Vegetation of Europe: Hierarchical floristic classification system of vascular plant, bryophyte, lichen, and algal communities. *Applied Vegetation Science*, *19 (Suppl. 1)*, 3–264. http://doi.org/Doi: 10.1111/avsc.12257

Myers-Smith, I. H., Forbes, B. C., Wilmking, M., Hallinger, M., Lantz, T., Blok, D., et al. (2011). Shrub expansion in tundra ecosystems: dynamics, impacts, and research priorities. *Applied Vegetation Science*, *6*. http://doi.org/10.1088/1748-9326/6/4/045509

Pajunen, A.M. (2009) Environmental and Biotic Determinants of Growth and Height of Arctic Willow Shrubs along a Latitudinal Gradient. *Arctic, Antarctic, and Alpine Research 41*, 478–485.

Pajunen, A., Virtanen, R., & Roininen, H. (2008). The effects of reindeer grazing on the composition and species richness. *Polar Biology*, *31*, 1233–1244.

Park, T., Ganguly, S., Tømmervik, H., Euskirchen, E. S., Høgda, K.-A., Karlsen, S. R., et al. (2016). Changes in growing season duration and productivity of northern vegetation inferred from long-term remote sensing data. *Applied Vegetation Science*, *11*(8), 084001. http://doi.org/10.1088/1748-9326/11/8/084001

Polunin, N. (1951). The real Arctic: suggestions for its delimitation, subdivision and characterization. *Journal of Ecology*, *39*, 308.

Prowse, T. D., Bring, A., Carmack, E. C., Holland, M. M., Instanes, A., Mård, J., et al. (2017). Freshwater. In AMAP (Ed.), *Snow, Water, Ice and Permafrost in the Arctic (SWIPA) 2017* (pp. 169–202). Oslo, Norway: Arctic Monitoring and Assessment Programme (AMAP).

R Development Core Team. (2013). R: A language and environment for statistical computing. Retrieved from http://www.R-project.org/.

Rannie, W. F. (1986). Summer air temperature and number of vascular species in arctic Canada. *Arctic*, *39*, 133–137.

Raynolds, M. K., Breen, A. L., Walker, D. A., Elven, R., Belland, R., Konstantinova, N., et al. (2013). The Pan-Arctic Species List (PASL). *Arctic Vegetation Archive Workshop, Krakow, Poland, 14-16 April 2013, CAFF Proceedings Series Report Nr. 10*, 92–95.

Raynolds, M. K., Comiso, J. C., Walker, D. A., & Verbyla, D. (2008). Relationship between satellite-derived land surface temperatures, arctic vegetation types, and NDVI. *Remote Sensing of Environment*, *112*(4), 1894. http://doi.org/10.1016/j.rse.2007.09.008

Razzhivin, V. Y. (1999). Zonation of vegetation in the Russian Arctic. In I. Nordal & V. Y. Razzhivin (Eds.), *The Species Concept in the High North - A Panarctic Flora Initiative* (Vol. I. Mat.-Naturv. Klasse Skrifter, pp. 113–130). Oslo.

Romanovsky, V., Isaksen, K., Drozdov, D., Anisimov, O., Instanes, A., Leibman, M., et al. (2017). Changing permafrost and its impacts. In AMAP (Ed.), *Snow, Water, Ice and Permafrost in the Arctic SWIPA 2017* (pp. 66–102). Oslo, Norway.

Sieg, B., Drees, B., & Daniëls, F. J. A. (2006). Vegetation and altitudinal zonation in continental West Greenland. *Meddelelser Om Grønland, Bioscience*, *57*, 1–93.

Smith, T. M., Reynolds, R. W., Peterson, T. C., & Lawrimore, J. (2008). Improvements to NOAA's Historical Merged Land–Ocean Surface Temperature Analysis (1880–2006). *Journal of Climate*, *21*(10), 2283–2296. http://doi.org/10.1175/2007JCLI2100.1

Soil Survey Staff. (1999). Soil taxonomy: A basic system of soil classification for making and Interpreting soil surveys (Vol. 436). Washington DC: U.S. Govt. Printing Office.

Stow, D. A., Hope, A., McGuire, D., Verbyla, D., Gamon, J., Huemmrich, F., et al. (2004). Remote sensing of vegetation and land-cover change in Arctic Tundra Ecosystems. *Remote Sensing of Environment*, *89*(3), 281–308. http://doi.org/10.1016/j.rse.2003.10.018

Tichý, L. (2002). JUICE, software for vegetation classification. *Journal of Vegetation Science*, *13*(3), 451–453. http://doi.org/10.1111/j.1654-1103.2002.tb02069.x

Tuhkanen, S. (1984). A circumboreal system of climatic-phytogeographical regions. *Acta Botanica Fennica*, *127*, 1.

Vowles, T., Lovehav, C., Molau, U., & Björk, R. G. (2017). Contrasting impacts of reindeer grazing in two tundra grasslands. *Applied Vegetation Science*, *12*(3), 034018. http://doi.org/10.1088/1748-9326/aa62af

Walker, D. A., Carlson, S., Frost, G. V., Matyshak, G. V., Leibman, M. E., Orekhov, P., et al. (2011a). *2010 Expedition to Krenkel Station, Hayes Island, Franz Josef Land Russia*. *AGC Data Report*. Fairbanks, AK: University of Alaska Fairbanks.

Walker, D. A., Daniëls, F. J. A., Matveyeva, N. V., Šibík, J., Walker, M. D., Breen, A. L., et al. (2018). Circumpolar Arctic Vegetation Classification. *Phytocoenologia*, *48*(2), 181–201. http://doi.org/10.1127/phyto/2017/0192.

Walker, D. A., Epstein, H. E., Leibman, M. E., Moskalenko, N. G., Kuss, H. P., Matyshak, G. V., et al. (2008a). *Data report of the 2007 Yamal expedition to Nadym, Laborovaya, and Vaskiny Dachi, Yamal Peninsula region, Russia*. *AGC Data Report*.

Walker, D. A., Epstein, H. E., Leibman, M. E., Moskalenko, N. G., Kuss, J. P., Matyshak, G. V., et al. (2009a). *Data Report of the 2007 and 2008 Yamal Expeditions: Nadym, Laborovaya, Vaskiny Dachi, and Kharasavey*. *AGC Data Report* (p. 133). Fairbanks, AK: University of Alaska.

Walker, D. A., Epstein, H. E., Raynolds, M. K., Kuss, P., Kopecky, M. A., Frost, G. V., et al. (2012a). Environment, vegetation and greenness (NDVI) along the North America and Eurasia Arctic transects. *Applied Vegetation Science*, *7*(1), 015504. http://doi.org/10.1088/1748-9326/7/1/015504

Walker, D. A., Frost, S., Timling, I., Raynolds, M. K., Matyshak, G., Frost, G. V., et al. (2012b). High cover, biomass, and NDVI of biological soil crusts on Hayes Island, Franz Josef Land, Russia. In K. M. Hinkel & V. P. Melnikov (Eds.), (Vol. 4, pp. 634–635). Presented at the Tenth International Conference on Permafrost, extended abstracts, Ekaterinburg, Russia.

Walker, D. A., Kuss, P., Epstein, H. E., Kade, A. N., Vonlanthen, C. M., Raynolds, M. K., & Daniëls, F. J. A. (2011b). Vegetation of zonal patterned-ground ecosystems along the North America Arctic bioclimate gradient. *Applied Vegetation Science*, *14*(4), 440–463. http://doi.org/10.1111/j.1654-109X.2011.01149.x

Walker, D. A., Orekhov, P., Frost, G. V., Matyshak, G., Epstein, H. E., Leibman, M. O., et al. (2009b). *The 2009 Yamal Expedition to Ostrov Belyy and Kharp, Yamal Region, Russia*. *AGC Data Report* (p. 63). Fairbanks, AK: University of Alaska Fairbanks.

Walker, D. A., Raynolds, M. K., & Gould, W. A. (2008b). Fred Daniëls, subzone A, and the North American Arctic Transect. *Abhandlungen Aus Dem Westfälischen Museum Für Naturkunde*, *70*(3/4), 387–400.

Walker, D. A., Raynolds, M. K., Daniëls, F. J. A., Einarsson, E., Elvebakk, A., Gould, W. A., et al. (2005). The Circumpolar Arctic Vegetation Map. *Journal of Vegetation Science*, *16*(3), 282. http://doi.org/10.1658/1100-9233(2005)016[0267:TCAVM]2.0.CO;2

Walker, M. D., Wahren, C. H., Hollister, R. D., Henry, G. H. R., Ahlquist, L. E., Alatalo, J. M., et al. (2006). Plant Community Responses to Experimental Warming across the Tundra Biome. *Proceedings of the National Academy of Sciences of the United States of America*, *103*(5), 1342–1346. http://doi.org/10.2307/30048374?ref=search-gateway:ac394e72cab959e78c49a3ea70dc25e6

Walker, M. D., Walker, D. A., & Auerbach, N. A. (1994). Plant communities of a tussock tundra landscape in the Brooks Range Foothills, Alaska. *Journal of Vegetation Science*, *5*, 866. http://doi.org/10.2307/3236198

Walter, H. (1954). Klimax und zonale Vegetation. *Angewandte Pflazensoziologie, Festschrift Aichinger*, *1*, 144–150.

Walter, H. (1973). Vegetation of the earth and ecological systems of the geo-biosphere. (J. Wieser, Trans.) (4 ed.). New York: Springer-Verlag.

Westhoff, V., & Van der Maarel, E. (1978). The Braun-Blanquet approach. In R. H. Whittaker (Ed.), *Classification of Plant Communities* (pp. 287–399). Den Haag.

Young, S. B. (1971). The vascular flora of St. Lawrence Island with special reference to floristic zonation in the arctic regions. *Contributions from the Gray Herbarium*, *201*, 11–115.

Yu, Q., Epstein, H. E., Walker, D. A., Frost, G. V., & Forbes, B. C. (2011). Modeling dynamics of tundra plant communities on the Yamal Peninsula, Russia, in response to climate change and grazing pressure. *Applied Vegetation Science*, *6*. http://doi.org/10.1088/1748-9326/6/4/045505

Yurtsev, B. A. (1994a). Latitudinal (zonal) and longitudinal (sectoral) phytogeographic division of the circumpolar arctic in relation to the structure of the vegetation map legend (Vol. 96, pp. 77–83). Presented at the Circumpolar Arctic Vegetation Mapping Workshop, Komarov Botanical Institute, St. Petersburg, Russia: USGS.

Yurtsev, B. A. (1994b). The floristic division of the Arctic. *Journal of Vegetation Science*, *5*(6), 765–776.

Figure captions

Figure 1. The Eurasia Arctic Transect and Arctic bioclimate subzones. Inset map shows circumpolar distribution of the subzones according to the Circumpolar Arctic Vegetation Map (CAVM Team 2003).

Figure 2. Mean soil textures for EAT loamy sites and sandy sites. a. Mean soil texture classes for each site plotted on a USDA soil-texture triangular (percent sand, silt, clay) with 12 size classes defined by the US Department of Agriculture (Soil Survey Staff, 1999) Each point represents the mean of 5 plots except for the FT-sandy (brown squares), which portray the mean values for hummocks (loamy sand) and inter-hummock (sand) plots. b. Sand, silt and clay percentages at loamy sites vs. summer warmth index (SWI_g). c. Sand, silt and clay percentages at sandy sites vs. summer warmth index (SWI_g).

Figure 3. Cluster analysis of EAT plots. The plot is based on similarity of species composition within the 76 plots using Sørensen's coefficient of distance measure and square root data transformation. The numbers on the left side of the diagram are consecutive plot numbers assigned in the Turboveg program. Corresponding plot field numbers are in the Supplement Information, Tables S3. All species (vascular plants, bryophytes and lichens) were included. Plots linked toward the left side of the diagram have high species similarity; linkages toward the right side of the diagram have low levels of similarity. The flexible-β group linkage method (β = -0.25) was used to hierarchically link the plots. The vertical red dashed line shows the second-optimal level of clustering based the Crispness of Classification approach (Botta-Dukát et al., 2005) available through the Optimclass function in JUICE (Tichý 2002), which resulted in the six optimal clusters (red numbers). The red line is where the line was adjusted to separate out cluster 6, which based on field observations was distinctive from cluster 5. Background colors correspond to the bioclimate subzones (A – Forest-tundra). Also shown are loamy and sandy groups of plots (black Roman labels), and micro-topographic groups of plots in patterned-ground complexes (italics).

Figure 4. Plant-growth-form cover and species-richness trends along the summer-warmth (SWI_g) gradient. **a-c.** Plant-growth-form cover in the layers of the plant canopy (tree and shrub, herb, and cryptogam). Left: Bar graphs of mean cover of plant growth forms at each location in loamy and sandy sites. Right: Trend lines of mean cover of major growth form groups (deciduous shrubs, evergreen shrubs, graminoids, forbs, bryophytes, and lichens) vs. SWI_g. **d.** Mean species richness vs. summer warmth (SWI_g). a. Mean total species richness on loamy and sandy sites. b. Mean species richness of major plant-growth-form (PFG) groups on loamy sites. c. Mean species richness of major plant-growth-form (PFG) groups on sandy sites. Equations of the trend lines are in Supplemental Information, Appendix S9.

Figure 5. Detrended Correspondence Analysis (DCA) ordination of EAT plots. a. Plot ordination with environmental joint plot. Units along the axes are sd units, an indicator of the amount of species turnover in the dataset. Four sd units are considered to represent approximately one complete species turnover. Plot symbols are color coded according to bioclimate subzones; shapes of symbols correspond to soil texture. Small letters (a, b) are microhabitats corresponding to patterned-ground features at the Nadym Site ND-2 (hummocks and inter-hummocks) and Ostrov Belyy Site OB-1 (nonsorted circles and inter-circle areas) and Site OB-2 (small nonsorted polygon centers and cracks). Red cluster numbers are according to clusters in Fig. 11. Joint-plot arrows denote direction and strength of correlations with environmental variables with $p \leq 0.05$. b. Species ordination. Centers of distributions are shown for the top five diagnostic taxa in each cluster. The alphabetic taxon codes are abbreviations containing the first four letters of the genus and first three letters of species names. Colors of taxa labels correspond to dominant bioclimate subzones of the clusters for which the taxa are diagnostic (Dark brown, cluster 1, FT-Forest; light brown, cluster 2, FT-tundra; red, cluster 4, subzone E & subzone D, sandy; green, cluster 5, subzone D, loamy & subzone C; dark blue, cluster 6, subzone B, loamy; light blue, cluster 7, subzone B, sandy; purple, cluster 3, subzone A. The joint plot includes the same variables as in a.

Table captions

Table 1. Study locations, site numbers, site names, microsites, geological settings, parent material, and dominant vegetation at each study site.

Table 2. Temperature and precipitation along the Eurasia Arctic Transect. Mean (1961-1990) July temperature, and precipitation data (columns 3 and 4) are from the nearest relevant climate stations. SWI is the sum of the monthly mean temperatures above freezing. The mean atmospheric SWI (SWI_a) (column 5) is calculated from the mean (1961-1990) station data, where available. Ground Summer Warmth Index (SWIg) (column 6) are calculated from AVHRR thermal bands for the 12.5-km pixels containing the EAT study locations. Value for SWI_g in the circumpolar Arctic subzones (column 7) are calculated using all circumpolar pixels within each subzone (Raynolds et al. 2008).

Table 3. Synoptic table of diagnostic taxa for the statistical clusters of mesic tundra vegetation plots along the Eurasia Arctic Transect. Values are frequency of the given plant taxon within the indicated cluster (see Fig. 3). Fidelity of diagnostic species was calculated using the phi coefficient (Chytrý et al.2002) for individual clusters compared to the full suite of clusters. Diagnostic taxa are ordered according to descending fidelity (modified phi values). Taxa with very high fidelity (modified phi ≥ 0.8) are highlighted in dark gray; those with high fidelity (modified phi > 50) are highlighted in gray. The second column in the table contains the plant growth form for each species. Codes for the growth forms are: bl - bryophyte, liverwort; bma - bryophyte, moss, acrocarpous; bmp - bryophyte, moss, pleurocarpous; bms -

bryophyte, moss, sphagnoid; fe - forb, erect; fm - forb, mat, cushion or rosette; gs - graminoid, sedge; gg - graminoid, grass; gr -graminoid, rush; lc - lichen, crustose; lfo - lichen, foliose; lfr - lichen, fruticose; sle - shrub, low, evergreen; sld- shrub, low, deciduous; sde - shrub, dwarf, evergreen; add - shrub, dwarf, deciduous; sde - shrub, dwarf, evergreen; tne - tree, needleleaf, evergreen; tnd - tree, needleleaf, deciduous; tbd - tree, broadleaf, deciduous; vs - vascular plant, seedless. See Supplementary Information, Appendix S6 for the full synoptic table containing all diagnostic and non-diagnostic taxa.

Supplemental Information Appendices

Appendix S1. Geological setting of the Yamal Peninsula.

Appendix S2. Typical plot layout.

Appendix S3. Eurasia Arctic Transect location and site descriptions.

Appendix S4. Eurasia Arctic Transect species cover-abundance data.

Appendix S5. Eurasia Arctic Transect environmental data.

Appendix S6. Full synoptic table.

Appendix S7. Diagnostic, constant, and dominant taxa for EAT clusters.

Appendix S8. Trends of selected soil and vegetation properties v. summer warmth index.

Appendix S9. Regression equations for trend lines of analyzed variables.
Appendix S10. Number of species per plot along the Eurasia Arctic Transect.

Appendix S11. Correlations between four axes of the DCA ordination and environmental variables.

Appendix S12. Lichen-rich tundra of Hayes Island.

Figures

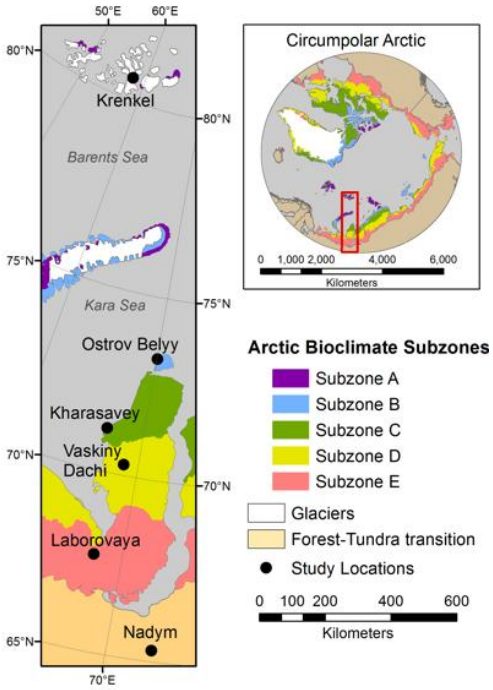

Figure 1. The Eurasia Arctic Transect and Arctic bioclimate subzones. Inset map shows circumpolar distribution of the subzones according to the Circumpolar Arctic Vegetation Map (CAVM Team 2003).

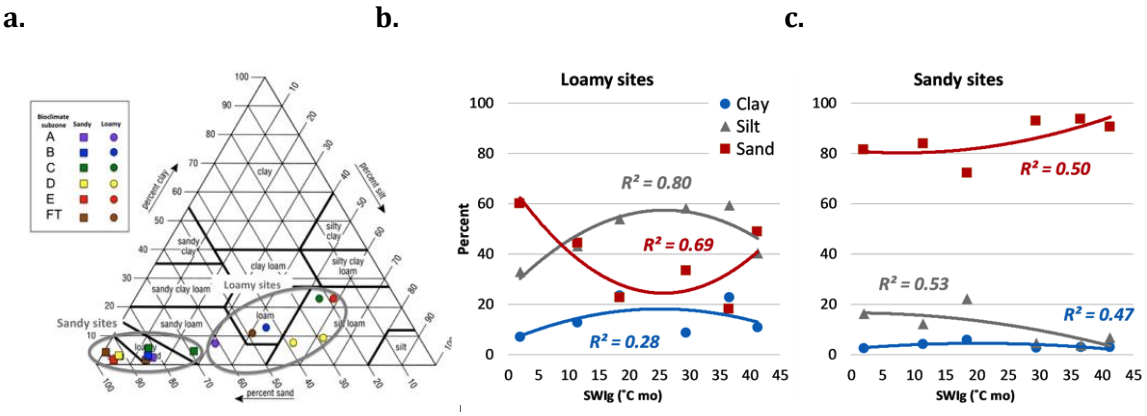

Figure 2. Mean soil textures for EAT loamy sites and sandy sites. a. Mean soil texture classes for each site plotted on a USDA soil-texture triangular (percent sand, silt, clay) with 12 size classes defined by the US Department of Agriculture (Soil Survey Staff, 1999) Each point represents the mean of 5 plots except for the FT-sandy (brown squares), which portray the mean values for hummocks (loamy sand) and inter-hummock (sand) plots. b. Sand, silt and clay percentages at loamy sites vs. summer warmth index (SWI_g). c. Sand, silt and clay percentages at sandy sites vs. summer warmth index (SWI_g).

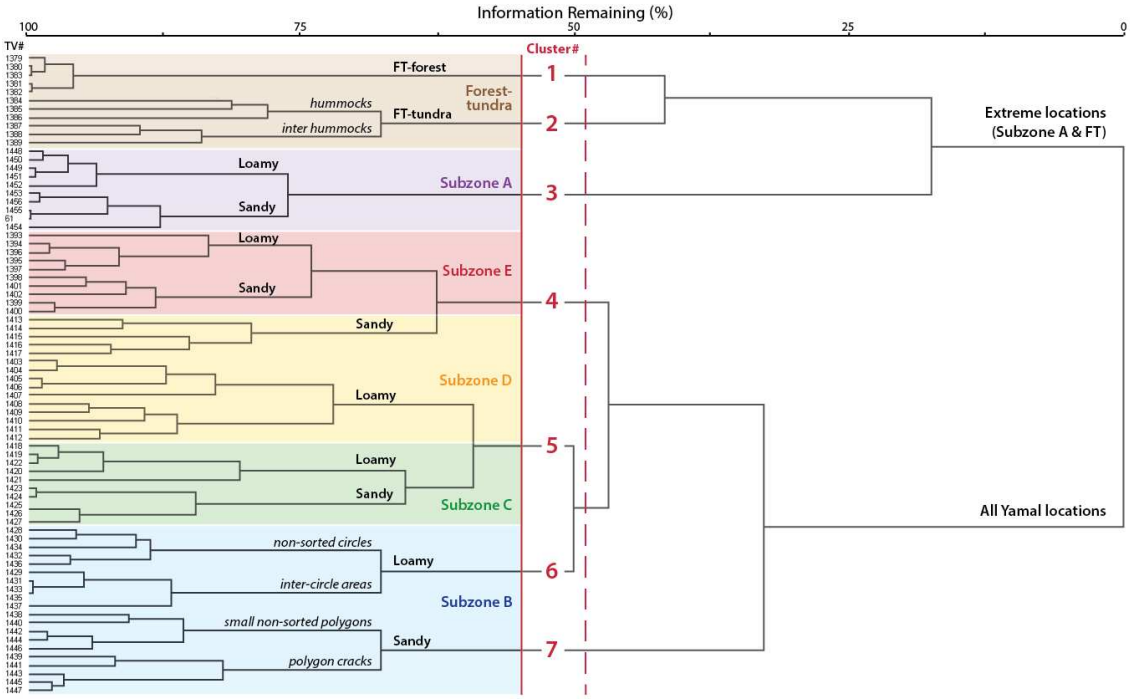

Figure 3. Cluster analysis of EAT plots. The plot is based on similarity of species composition within the 76 plots using Sørensen's coefficient of distance measure and square-root data transformation. The numbers on the left side of the diagram are consecutive plot numbers assigned in the Turboveg program. Corresponding plot field numbers are in the Supplement Information, Tables S3. All species (vascular plants, bryophytes and lichens) were included. Plots linked toward the left side of the diagram have high species similarity; linkages toward the right side of the diagram have low levels of similarity. The flexible-β group linkage method (β = -0.25) was used to hierarchically link the plots. The vertical red dashed line shows the second-optimal level of clustering based the Crispness of Classification approach (Z. Botta-Dukát et al., 2005) available through the Optimclass function in JUICE (Tichý 2002), which resulted in the six optimal clusters (red numbers). The red line is where the line was adjusted to separate out cluster 6, which based on field observations was distinctive from cluster 5. Background colors correspond to the bioclimate subzones (A – Forest-tundra). Also shown are loamy and sandy groups of plots (black Roman labels), and micro-topographic groups of plots in patterned-ground complexes (italics).

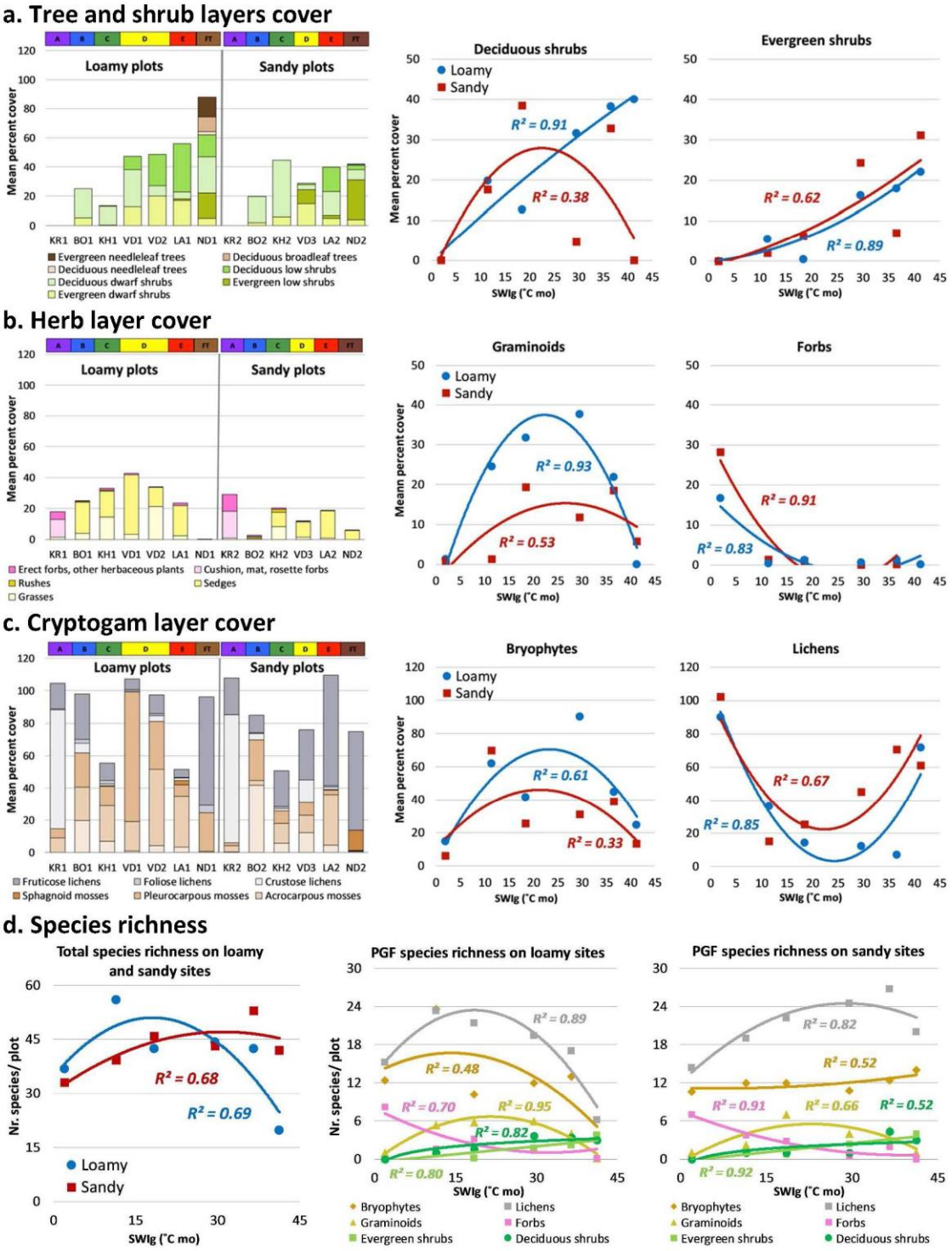

Figure 4. Plant-growth-form cover and species-richness trends along the summer-warmth (SWI_g) gradient. **a-c.** Plant-growth-form cover in the layers of the plant canopy (tree and shrub, herb, and cryptogam). Left: Bar graphs of mean cover of plant growth forms at each location in loamy and sandy sites. Right: Trend lines of mean cover of major growth form groups (deciduous shrubs, evergreen shrubs, graminoids, forbs, bryophytes, and lichens) vs. SWI_g. **d.** Mean species richness vs. summer warmth (SWI_g). a. Mean total species richness on loamy and sandy sites. b. Mean species richness of major plant-growth-form (PFG) groups on loamy sites. c. Mean species richness of major plant-growth-form (PFG) groups on sandy sites. Equations of the trend lines are in Supplemental Information, Appendix S9.

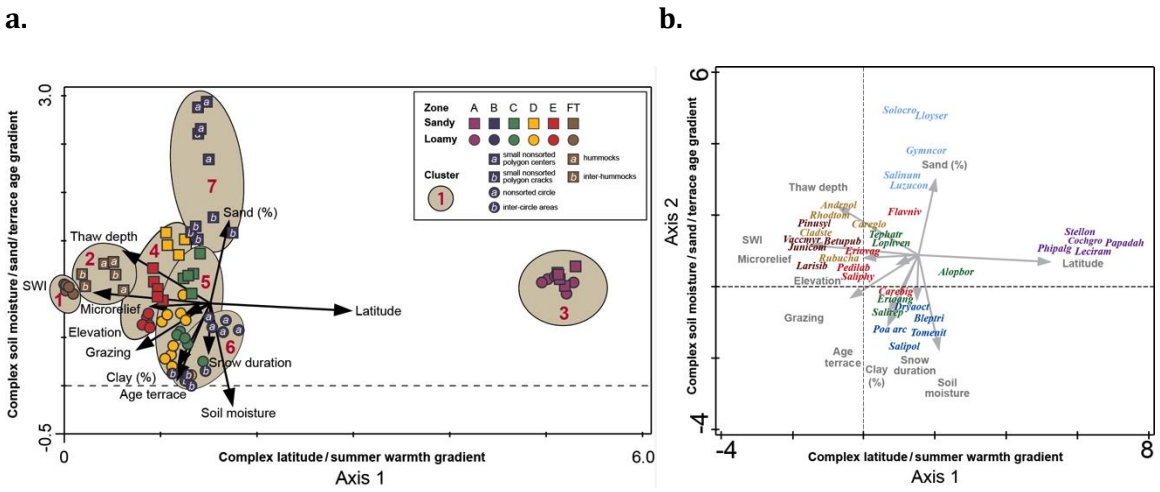

Figure 5. Detrended Correspondence Analysis (DCA) ordination of EAT plots. a. Plot ordination with environmental joint plot. Units along the axes are sd units, an indicator of the amount of species turnover in the dataset. Four sd units are considered to represent approximately one complete species turnover. Plot symbols are color coded according to bioclimate subzones; shapes of symbols correspond to soil texture. Small letters (a, b) are microhabitats corresponding to patterned-ground features at the Nadym Site ND-2 (hummocks and inter-hummocks) and Ostrov Belyy Site OB-1 (nonsorted circles and inter-circle areas) and Site OB-2 (small nonsorted polygon centers and cracks). Red cluster numbers are according to clusters in Fig. 11. Joint-plot arrows denote direction and strength of correlations with environmental variables with $p \leq 0.05$. b. Species ordination. Centers of distributions are shown for the top five diagnostic taxa in each cluster. The alphabetic taxon codes are abbreviations containing the first four letters of the genus and first three letters of species names. Colors of taxa labels correspond to dominant bioclimate subzones of the clusters for which the taxa are diagnostic (Dark brown, cluster 1, FT-Forest; light brown, cluster 2, FT-tundra; red, cluster 4, subzone E & subzone D, sandy; green, cluster 5, subzone D, loamy & subzone C; dark blue, cluster 6, subzone B, loamy; light blue, cluster 7, subzone B, sandy; purple, cluster 3, subzone A. The joint plot includes the same variables as in a.

Tables

Table 1. Study locations, site numbers, site names, microsites, geological settings, parent material, and dominant vegetation at each study site.

Location	Coordinates	Bio-climate subzone	Site	Geological setting[1], parent material	Microsite	Plot field numbers	Dominant vegetation
Krenkel	80˚ 37' N, 58˚ 03' E	A	KR-1, Loamy	Deluvial slope or perhaps old marine terrace at 30 m, sands		KR_RV_60-64	*Papaver dahlianum* spp. *polare, Stellaria edwardsii, Cetrariella delisei, Ditrichum flexicaule,* biological soil crust, cushion-forb, lichen, moss tundra
			Kr-2 Sandy	Recent marine terrace at 10 m, marine sands		KR_RV_65-69	*Papaver dahlianum* spp. *polare, Stellaria edwardsii, Cetrariella delisei*, biological soil crust, cushion-forb, lichen, moss tundra
Ostrov Belyy	73°19' N, 70°03' E	B	OB-1, loamy	Marine terrace II, alluvial-marine sediments, loamy facie of mixed sands and silts	OB-1a, Non-sorted circles	OB_RV_49a-53a	*Carex bigelowii, Calamagrostis holmii, Salix polaris, Hylocomium splendens,* graminoid, prostrate dwarf-shrub, moss tundra
					OB-1b, Inter-circle areas	OB_RV_49b-53b	*Dryas integrifolia, Arctagrostis latifolia, Racomitrium lanuginosum, Ochrolechia frigida,* prostrate dwarf-shrub, crustose-lichen barren
			OB-2, Sandy	Marine terrace I, alluvial-marine sediments, sands	OB-2a, Small nonsorted polygons centers	OB_RV_54a-58a	*Gymnomitrion corallioides-Salix nummularia-Luzula confusa-Ochrolechia frigida,* liverwort, dwarf-shrub, graminoid, lichen tundra
					OB-2b, Polygon cracks	OB_RV_53b-58b	*Racomitrium lanuginosum, Salix nummularia,* moss, prostrate dwarf-shrub tundra
Khara-savey	71°12' N, 66°56' E	C	KH-1, loamy	Marine terrace II, marine silts		KH_RV_40-44	*Carex bigelowii, Calamagrostis holmii, Salix polaris, Dicranum elongatum, Cladonia spp.,* graminoid, prostrate dwarf-shrub, moss tundra
			KH-2a, sandy	Marine terrace I, marine silts		KH_RV_45-46	*Carex bigelowii, Salix nummularia, Dicranum sp., Cladonia spp.,* graminoid, prostrate dwarf-shrub, moss, lichen tundra
			KH-2b, sandy	Marine terrace II, marine sands and silts		KH_RV_47-49	*Salix nummularia, Luzula confusa, Polytrichum strictum, Sphaerophorus globosus,* prostrate dwarf-shrub, graminoid, moss, lichen tundra
Vaskiny Dachi	70˚ 17' N, 68˚ 54' E	D	VD-1, loamy	Coastal-marine plain terrace IV, , mixed Alluvial sands and marine silts		VD_RV_25-29	*Carex bigelowii, Vaccinium vitis-idaea, Hylocomium splendens,* sedge, dwarf-shrub, moss tundra
			VD-2, loamy	Fluvial-marine terrace III, mixed alluvial sands and marine silts		VD_RV_30-34	*Betula nana, Calamagrostis holmii, Aulacomnium turgidum,* dwarf-shrub, graminoid, moss tundra
			VD-3, sandy	Fluvial terrace II, alluvial and eolian reworked sands		VD_RV_35-39	*Vaccinium vitis-idaea, Cladonia arbuscula, Racomitrium lanuginosum,* prostrate dwarf-shrub, sedge, lichen, tundra
Laboro-vaya	67° 42' N, 68° 01' E	E	LA-1, loamy	Glacial terrace, glacial silt		LA_RV_15-19	*Carex bigelowii, Betula nana, Aulacomnium palustre,* sedge, dwarf-shrub, moss tundra
			LA-2, sandy	Recent (< 10 kya) alluvial terrace of stream, alluvial sand		LA_RV_20-21	*Betula nana, Vaccinium vitis-idaea, Sphaerophorus globosus, Polytrichum strictum,* prostrate dwarf-shrub, lichen tundra
Nadym	65˚ 19' N, 72˚ 53' E	Forest-tundra transition	ND-1, loamy, forest	Fluvial terrace II, alluvial loamy sands		ND_RV_01 to 05	*Pinus sylvestris, Betula tortuosa, Rhododendron tomentosum, Cladonia stellaris,* dwarf-shrub, lichen woodland
			ND-2, sandy, tundra	Fluvial terrace III, alluvial sands	ND-2a, Hum-mocks	ND_RV_06-08	*Rhododendron tomentosum, Betula nana, Cladonia stellaris,* dwarf-shrub, lichen tundra
					ND-2b, Inter-hum-mocks	ND_RV_09-11	*Cladonia stellaris, Carex glomerata,* lichen tundra

[1] Marine and alluvial terrace numnbers (see Fig. 2), approximate elevations above mean sea level on the Yamal Peninsula, approximate ages:

Marine terrace I, 7-12 m a.s.l., Sartansky-age (Last Glacial Maximum, Late Wiechselian), ≈ 10-25 ka
Marine terrace II, 10-25 m a.s.l., Karginsky-Zyransky-age (Middle Weichselian), ≈ 25-75 ka
Marine terrace III, 26-40 m a.s.l., Ermanovsky-age (Early Weichselian), ≈ 75-117 ka
Marine terrace IV, 40-45 m a.s.l., Kazantsevskaya-age (Eemian interglacial), ≈ 117-130 ka
Marine terrace V, 45-58 m a.s.l., Salekhardskaya age (Saalian), ≈130- 200 ka

Table 2. Temperature and precipitation along the Eurasia Arctic Transect. Mean (1961-1990) July temperature, and precipitation data (columns 3 and 4) are from the nearest relevant climate stations. SWI is the sum of the monthly mean temperatures above freezing. The mean atmospheric SWI (SWI_a) (column 5) is calculated from the mean (1961-1990) station data, where available. Ground Summer Warmth Index (SWIg) (column 6) are calculated from AVHRR thermal bands for the 12.5-km pixels containing the EAT study locations. Value for SWI_g in the circumpolar Arctic subzones (column 7) are calculated using all circumpolar pixels within each subzone (Raynolds et al. 2008).

Bioclimate subzone	EAT study location	Mean July Temp. (1961-1990, ˚C)[1]	Mean annual precipitation (1961-1990, mm)[1]	Mean SWI_a at local climate station (1961-1990, ˚C mo)[1]	Mean SWI_g for 12.5-km km pixel containing the location (˚C mo)	Mean SWI_g for Circum-polar Arctic subzones (Mean ± s.d., ˚C mo)
A	Krenkel	1	282	1.1	2.0	8.2 ± 3.4
B	Ostrov Belyy	5.6	258	11	11.5	12.6 ± 5.8
C	Kharasavey	7.2*	310*	18.6*	18.5	19.8 ± 5.1
D	Vaskiny Dachi	ND	ND	ND	29.6	27.0 ± 4.9
E	Laborovaya	ND	ND	ND	36.6	33.2 ± 4.4
FT-transition	Nadym	15.8	479	43	41.3	ND

[1] Leibman et al., 2012

* Data from Mare-/Sale, closest coastal station to Kharasavey, 100 km south.

Table 3. Synoptic table containing diagnostic taxa for statistical clusters of mesic tundra vegetation plots along the Eurasia Arctic Transect. Values are frequency of the given plant taxon within the indicated cluster (see Fig. 11). Fidelity of diagnostic species was calculated using the phi coefficient (Chytrý et al., 2002) for individual clusters compared to the full suite of clusters. Diagnostic taxa are ordered according to descending fidelity (modified phi values). Taxa with very high fidelity (modified phi ≥ 0.8) have frequency values highlighted in dark gray; those with high fidelity (modified phi > 50) are highlighted in light gray. The second column in the table contains the plant growth form for each species: **bl**, bryophyte, liverwort; **bma**, bryophyte, moss, acrocarpous; **bmp**, bryophyte, moss, pleurocarpous; **bms**, bryophyte, moss, sphagnoid; **fe**, forb, erect; **fm**, forb, mat, cushion or rosette; **gs**, graminoid, sedge; **gg**, graminoid, grass; **gr**, graminoid, rush; **lc**, lichen, crustose; **lfo**, lichen, foliose; **lfr**, lichen, fruticose; **sle**, shrub, low, evergreen; **sld**, shrub, low, deciduous; **sde**, shrub, dwarf, evergreen; **sdd**, shrub, dwarf, deciduous; **tne**, tree, needleleaf, evergreen; **tnd**, tree, needleleaf, deciduous; **tbd**, tree, broadleaf, deciduous; **vs**, vascular plant, seedless.

Cluster nr.		**1**	**2**	**4**	**5**	**6**	**7**	**3**
Subzone(s) (soil texture)		**FT(lom)**	**FT(snd)**	**E+D(snd)**	**D(lom)+C**	**B(lom)**	**B(snd)**	**A**
Number of plots		**5**	**6**	**15**	**20**	**10**	**10**	**10**
Diagnostic taxa for cluster 1:	**Growth form**							
Pinus sylvestris	tne	100	.					
Betula pubescens	tbd	100	.					
Larix sibirica	tnd	100	.					
Vaccinium myrtillus	sdd	100	.					
Juniperus communis	sle	80	.					
Peltigera malacea	lfo	60	.					
Pleurozium schreberi	bmp	100	17	47	5	.	.	
Peltigera leucophlebia	lfo	100	.	13	50	20	.	
Cladonia stellaris	lfr	100	83	20	.	.	.	
Empetrum nigrum	sde	100	17	80	10	.	.	
Vaccinium uliginosum	sdd	100	33	67	15	.	.	
Diagnostic taxa for cluster 2;								
Carex globularis	gs	.	100	.	.	.	.	.
Andromeda polifolia	sde	.	83	7	.	.	.	.
Rubus chamaemorus	sdd	.	83	7	.	.	.	.
Rhododendron tomentosum s. *tomentosum*	sle	100	100	73	.	.	.	.
Diagnostic taxa for cluster 4:								
Flavocetraria nivalis	lfr	.	.	93	25	.	.	.
Salix phylicifolia	sld	.	.	67	10	.	.	.
Eriophorum vaginatum	gs	.	17	87	25	.	.	.
Pedicularis labradorica	fe	.	.	53	.	.	.	.
Asahinea chrysantha	lfr	.	.	40	.	.	.	.
Pertusaria dactylina	lc	.	.	47	.	.	10	.
Cladonia grayi	lfr	.	.	40	5	.	.	.
Schljakovia kunzeana	bl	.	.	33	.	.	.	.

Luzula wahlenbergii	gr	.	.	33	.	.	.	.
Diagnostic taxon for clusters 5 & 6:								
Arctagrostis latifolia	gg	.	.	20	95	100	10	.
Diagnostic taxa for cluster 5:								
Lophozia ventricosa	bl	.	.	40	80	.	.	.
Alopecurus borealis	gg	.	.	.	60	.	.	10
Salix reptans	sdd	.	.	13	55	.	.	.
Eriophorum angustifolium	gs	.	.	27	60	.	.	.
Tephroseris atropurpurea	fe	.	.	7	45	.	.	.
Peltigera canina	lfo	.	.	.	35	.	.	.
Peltigera aphthosa	lfo	.	.	.	40	10	.	.
Lichenomphalia hudsoniana	lfo	.	.	.	30	.	.	.
Diagnostic taxa for cluster 6:								
Blepharostoma trichophyllum	bl	.	.	.	5	100	.	.
Salix polaris	sdd	.	.	.	50	100	.	.
Tomentypnum nitens	bmp	.	.	13	20	90	.	.
Dryas octopetala	sde	.	.	.	40	100	50	.
Poa arctica	gg	.	.	7	40	80	.	.
Juncus biglumis	gr	.	.	.	.	60	20	.
Bryum cyclophyllum	bma	.	.	.	.	40	.	.
Stellaria longipes	fe	.	.	.	25	60	.	.
Sphenolobus minutus	bl	.	.	73	80	100	20	.
Diagnostic taxa for cluster 7:								
Pogonatum dentatum	bma	.	.	13	.	.	80	.
Oxyria digyna	fm	.	.	.	.	.	80	20
Gymnomitrion corallioides	bl	.	.	33	25	10	100	.
Luzula confusa	gr	.	.	.	60	10	100	.
Salix nummularia	sdd	.	.	27	50	.	100	.
Lloydia serotina	fe	.	.	.	.	.	50	.
Solorina crocea	lfo	.	.	.	.	.	50	.
Polytrichum piliferum	bma	.	.	7	.	10	50	.
Pohlia crudoides	bma	.	.	7	.	.	40	.
Gowardia nigricans	lfr	.	.	40	60	20	90	.
Diagnostic taxa for cluster 3:								
Stellaria longipes taxon edwardsii	fe	.	.	.	.	.	.	100
Papaver dahlianum agg. (*P. cornwallisense*)	fm	.	.	.	.	.	.	100
Phippsia algida	gg	.	.	.	.	.	.	100
Cochlearia groenlandica	fm	.	.	.	.	.	.	100
Lecidea ramulosa	lc	.	.	.	.	.	.	100
Orthothecium chryseum	bmp	.	.	.	.	10	.	100

Cladonia pocillum	lfr	.	.	.	.	10	.	100
Cetrariella delisei	lfr	.	.	20	.	.	.	100
Cerastium nigrescens v. *laxum*	fm	.	.	.	.	.	.	80
Fulgensia bracteata	lc	.	.	.	.	.	.	80
Saxifraga cernua	fe	.	.	.	5	.	.	80
Draba subcapitata	fm	.	.	.	.	.	20	90
Cirriphyllum cirrosum	bmp	.	.	.	.	.	.	70
Cerastium regelii	fm	.	.	.	.	10	.	70
Encalypta alpina	bma	.	.	.	.	.	.	60
Solorina bispora	lfo	.	.	.	.	.	.	60
Bryum rutilans	bma	.	.	.	.	.	.	60
Saxifraga cespitosa	fm	.	.	.	.	.	.	60
Distichium capillaceum	bma	.	.	.	.	30	.	80
Cetraria aculeata	lfr	.	.	.	.	.	20	70
Pohlia cruda	bma	.	.	.	.	40	.	80
Gowardia arctica	lfr	.	.	.	.	.	.	50
Saxifraga oppositifolia	fm	.	.	.	.	.	.	50
Cladonia symphycarpia	lfr	.	.	.	.	.	.	50
Stereocaulon rivulorum	lfr	.	.	.	.	.	.	50
Polytrichastrum alpinum	bma	.	.	.	30	10	60	100
Bartramia ithyphylla	bma	.	.	.	.	.	10	50
Callialaria curvicaulis	bmp	.	.	.	.	.	.	40
Campylium stellatum v. *arcticum*	bmp	.	.	.	.	.	.	40
Ditrichum flexicaule	bma	.	.	.	5	40	.	70
Protopannaria pezizoides	lc	.	.	.	5	.	.	40